Sensitivity of Wind Farm Wake Steering Strategies to Analytical Wake Models

F. Gori, A. Wynn & S. Laizet
Department of Aeronautics, Imperial College London, London, United Kingdom

ABSTRACT: The aerodynamic interactions between wind turbines arranged in farm layout lead to annual energy production losses ranging from 10% to 30%. Wake steering represents a promising strategy in wind farm control for power loss mitigation. The purpose of this work is to assess the sensitivity of optimal wake steering strategies to both analytical wake model choice and optimisation parameters. Using the FLOw Redirection and Induction in Steady State (FLORIS) framework, different wake models are employed to optimise a 4×4 farm layout for power maximisation. Model comparison findings indicate significant discrepancies in absolute power predictions for optimal set-points, as well as in optimal decision variables, with different or even opposite optimal yaw angle settings. Initialisation sensitivity results show that solutions corresponding to local extrema lead to potential power losses up to 14% compared to the global maximum for power production. Moreover, wind farm power function is observed to be multi-modal and discontinuous, suggesting that care must be taken when using gradient-based methods in wake steering optimisation.

1 INTRODUCTION

Wind energy is gaining international momentum around the globe, driven by the urgent environmental need to reduce carbon emissions and the significant decrease in the cost of renewables. One of the outstanding challenges is the mitigation of aerodynamic interactions between wind turbines arranged in a farm layout. Aerodynamic interactions, or wake losses, can lead to a decrease in annual energy production of a wind farm of between 10% and 30% (Barthelmie et al. 2009, Barthelmie et al. 2010, Nygaard 2014), reaching over 50% in certain wind conditions (Nilsson et al. 2015). Active wake control plays a major role in reducing the drawbacks of wake losses. Although various promising strategies have recently been developed (see Kheirabadi and Nagamune (2019) and Houck (2021) for comprehensive reviews), the current study focuses on wake steering, namely the intentional misalignment of upstream turbines to deflect the generated wakes in the cross-stream direction. Multiple campaigns, including high-fidelity simulations (Fleming et al. 2015, Fleming et al. 2018), wind tunnel testing (Campagnolo et al. 2016, Bastankhah et al. 2019), and field testing (Howland et al. 2019), have highlighted significant potential for wake steering to enable both power loss reduction and fatigue loads mitigation.

The development of analytical wake models to efficiently describe wind farm flow physics has received significant attention. Due to computational complexity, computational fluid dynamics (CFD) methods, such as large-eddy simulation (LES), limit the potential to use model-based open-loop and feedback control. Open-loop approaches rely on pre-computed lookup tables and assume stationary wind farm statistics. Feedback control accounts for variations in wind farm behaviour as a function of time by performing online optimisation at each time step. Analytical wake models represent an alternative approach to CFD. Computationally efficient steady formulations are developed to capture only the most dominant wake characteristics.

Various steady wake model formulations for predicting streamwise velocity include a mass-conserving top-hat distribution by Jensen (1983), a modification with top-hat wake zones by Gebraad et al. (2014), and a mass and momentum conserving top-hat formulation by Frandsen et al. (2006). More recently, Bastankhah and Porté-Agel (2014) applied a self-similar Gaussian distribution with further developments to include atmospheric stability (Abkar and Porté-Agel 2015, Niayifar and Porté-Agel 2016), added turbulence intensity due to upstream turbines (Niayifar and Porté-Agel 2016), and three-dimensional wake expansion rates (Abkar and Porté-Agel 2015). Additional formulations include the prediction of yaw added turbulence intensity and secondary steering effects (King et al. 2021), near-wake corrections (Qian and Ishihara 2018, Blondel and

Cathelain 2020), and a double-Gaussian streamwise velocity distribution (Schreiber et al. 2020).

In yawed conditions, deflection models are necessary to quantify the cross-stream wake deflection caused by the thrust unbalance on the misaligned rotor. Jiménez et al. (2009) proposed a mass and momentum conserving relationship to calculate the wake skew angle where a top-hat distribution is assumed for the wake streamwise velocity. Bastankhah and Porté-Agel (2016) and Qian and Ishihara (2018) developed model formulations based on vortex theory and a Gaussian distribution of the velocity deficit. Gaussian and top-hat skew angle distributions are assumed, respectively. Shapiro et al. (2018) treated the yawed turbines as a porous lifting surface with an elliptic distribution. Prandtl's lifting theory is used to compute wake skew angle. Shapiro et al. (2020) proposed an analytical expression for yawed turbine where the circulation decay of counter-rotating vortex cores is computed. More recent developments include the modelling of secondary steering effects (Zong and Porté-Agel 2020, King et al. 2021) and curled wake shape (Bastankhah et al. 2022).

Although validations of wake and deflection models are included in the respective publications, recent investigations (Archer et al. 2018, Stieren and Stevens 2021, Yang and Najafi 2021, Hegazy et al. 2022) have been conducted to compare wake model predictions against high-fidelity simulation results and field measurements in a wider range of conditions, including large farm layouts and farm-to-farm interaction. While the main focus of these comparisons is the model discrepancies in absolute power predictions, the current work also aims to determine, in an optimisation setting, the model discrepancies in optimal decision variables (turbine yaw angles for wake steering). In addition, the behaviour of wake models and their impact on the choice of optimisation algorithms are assessed by performing a sensitivity analysis to initialisation.

Using the open-source `FLORIS` tool, different wake models are used to optimise a 4×4 farm layout for power maximisation. The main purpose is to investigate and assess the general sensitivity of wake steering strategies to both the choice of analytical wake models and optimisation parameters. An extended version of the current work can be found in Gori et al. (2022), where an in-depth initialisation sensitivity analysis, a farm power function investigation, and a comparison between a gradient-based and a global optimiser are conducted on a 5×5 wind farm layout.

The remainder of the paper is organised as follows. In Section 2, `FLORIS` and the wake velocity deficit models are introduced. An overview of the optimisation setup is provided in Section 2.3. Optimisation results are presented and discussed in Section 3. Finally, conclusions are provided in Section 4.

2 METHODOLOGY

2.1 *FLORIS*

The investigation presented is carried out using `FLORIS` tool (version 2.4) of the National Renewable Energy Laboratory (NREL). The steady wake models compared are Jensen, Multi-zone, Gaussian, and Gauss-Curl Hybrid (GCH). The choice is motivated by the different levels of complexity in the model formulations, physical description capabilities, empirical parameter dependencies, and computational requirements of the selected analytical wake models. The aim is to assess a generalised sensitivity of wake steering strategies to the choice of wake models, as well as identify key model differences in a control context. All of the compared models are widely used by the wind energy community in optimisation and control studies (Kheirabadi and Nagamune 2019). Refer to Section 2.2 for additional details on the wake model formulations and the applied deflection models.

As a brief overview of `FLORIS` modelling structure, given an initial atmospheric inflow, wind farm layout, turbine geometry, and operational conditions, the steady streamwise velocity deficit is calculated for each turbine. After applying additional added turbulence intensity considerations and a deflection to the wake of yawed turbines, streamwise velocity deficits are combined by a superposition model. In the current work, all models share the sum of the squares freestream superposition (SOSFS) model developed by Katic et al. (1987). Given a mean free stream velocity U_∞ and the wake streamwise velocity induced by wind turbine i in stand-alone conditions u_w^i, the combined wake velocity U_w, dependant on the three spatial dimensions (x, y, z), is defined as

$$U_w(x,y,z) = U_\infty - \sqrt{\sum_i \left(U_\infty - u_w^i(x,y,z)\right)^2}\,. \quad (1)$$

Regarding wind farm power calculations, turbines' operational profiles are provided by lookup tables for power and thrust coefficients (C_P and C_T, respectively) generated by `FAST` (Fatigue, Aerodynamics, Structures, and Turbulence) aeroelastic simulator by NREL. Furthermore, the power reduction due to yaw actuation is included by applying a $\cos(\gamma)^w$ correction to the average rotor velocity, where γ is the turbine yaw angle to the inflow direction, and w is a tunable parameter that matches power losses due to yaw misalignment observed in simulations ($w = 0.627$ in the current work (Fleming et al. 2017)).

2.2 *Wake models*

2.2.1 *Jensen*

The Jensen model (Jensen 1983) is a mass-conserving steady wake model widely used in industry. It is coupled with the Jimenez deflection model (Jiménez et al.

2009). The main assumptions are the conservation of the cross-stream integral of the streamwise velocity deficit as the wake linearly expands downstream and the velocity deficit being simply a function of the downstream distance x. The latter implies a uniform velocity deficit in the wake.

Defining a cylindrical coordinate system at the rotor hub of the first upstream turbine with r and x referring to the radial and streamwise distances, respectively, the mean streamwise velocity deficit induced by a turbine with diameter D, assumed to operate at an induction factor a, can be expressed as

$$\delta u(x,r) = \begin{cases} 2a\left(\frac{D}{D+2kx}\right)^2, & \text{if } r \leq \frac{D+2kx}{2} \\ 0, & \text{otherwise} \end{cases} , \tag{2}$$

where k is the dimensionless expansion coefficient.

2.2.2 *Multi-zone*

The Multi-zone model, developed by Gebraad et al. (2014), is a modification of the Jensen model where within a turbine wake, three zones q are defined: near wake zone ($q = 1$), far wake zone ($q = 2$), and mixing wake zone ($q = 3$). They are assumed to expand linearly with downstream distance x. Different expansion rates are determined based on the tuned model parameters k_e and $m_{e,q}$. For a turbine operating at an induction factor a and yaw angle γ, the mean streamwise velocity deficit can be defined as

$$\delta u(x,r) = 2ac(x,r) \, . \tag{3}$$

Depending on the radial position r, the local decay coefficient c can be defined for each wake zone c_q as

$$c_q(x) = \left[\frac{D}{D + 2k_e m_{U,q}(\gamma)\, x}\right]^2 , \tag{4}$$

where $m_{U,q}$ is an empirically derived coefficient.

For additional details on the formulation of the wake model, refer to Gebraad et al. (2014). As for the Jensen model, Multi-zone is coupled with the Jimenez deflection model (Jiménez et al. 2009).

2.2.3 *Gaussian*

The Gaussian model is a steady, mass and momentum conserving wake model introduced by several recent publications (Bastankhah and Porté-Agel 2014, Abkar and Porté-Agel 2015, Bastankhah and Porté-Agel 2016, Niayifar and Porté-Agel 2016, Dilip and Porté-Agel 2017). In the wake velocity deficit description, atmospheric stability and added turbulence intensity due to upstream turbines are considered. The Gaussian model is coupled with the deflection model developed by Bastankhah & Porté-Agel (2016).

The streamwise velocity deficit formulation in the far wake is based on a simplification of the Navier-Stokes equations, where a Gaussian distribution is imposed based on the self-similarity theory used in free shear flows. Velocity deficit is dependent on the three spatial dimensions (x, y, z), and a linear wake expansion is assumed. Considering a three-dimensional space with the origin at the centre of the turbine rotor, the streamwise velocity deficit in the far wake is defined as

$$\delta u(x,y,z) = Ce^{-(y-\delta)^2/2\sigma_y^2} e^{-(z-z_{\mathrm{h}})^2/2\sigma_z^2} , \tag{5}$$

where C is the velocity deficit at the wake centre, δ the wake deflection, z_h the turbine hub height, and σ_y and σ_z the standard deviations of the Gaussian velocity deficit at each streamwise location, representing the wake width in the cross-stream and vertical direction.

The velocity deficit at the wake centre C can be expressed by

$$C(x) = 1 - \sqrt{1 - \frac{C_T \cos\gamma}{8\left(\sigma_y \sigma_z / D^2\right)}} , \tag{6}$$

where C_T is the turbine thrust coefficient. Standard deviations σ_y and σ_z are defined as

$$\sigma_y(x) = k_w(x - x_0) + \sigma_{y0} , \tag{7}$$

$$\sigma_z(x) = k_w(x - x_0) + \sigma_{z0} . \tag{8}$$

Quantities with a "0" suffix represent wake properties at the far wake onset (end of the near wake), while the k_w parameter defines the linear wake expansion rate, dependent on tuning parameters, ambient turbulence intensity, and added turbulence intensity due to upstream turbines. For additional details on the far wake onset quantities and turbulence intensity calculations, refer to Bastankhah and Porté-Agel (2016) and Niayifar and Porté-Agel (2016), respectively.

2.2.4 *Gauss-Curl Hybrid*

The Gauss-Curl Hybrid (GCH) model (King et al. 2021) extends the capabilities of the Gaussian model by implicitly modelling wake rotation and counter-rotating vortices with analytical approximations. Hence, wake asymmetry, added yaw-based wake recovery, and secondary steering effects are described. For the sake of brevity, an overview of the model is provided. For the full mathematical formulation, refer to King et al. (2021). As for the Gaussian model, GCH is coupled with the deflection model developed by Bastankhah & Porté-Agel (2016).

Added wake recovery due to turbine misalignment is computed by increasing turbulence intensity, directly affecting the wake linear expansion rate k_w. Due to the enhancement of turbulent mixing, an additional I_{mixing} term is included in the turbulence intensity formulation based on approximated cross-stream and vertical velocity components. As a result, the total turbulence intensity I_{total} is defined as

$$I_{\text{total}} = I + \phi I_{\text{mixing}} , \tag{9}$$

where I accounts for ambient turbulence intensity and added turbulence intensity due to upstream turbines, and ϕ is a tunable parameter.

Secondary steering effects refer to the wake deflection and deformation experienced by a downstream turbine without yaw misalignment due to the interaction between the vortices generated upstream by yaw-actuated turbines and the wake rotation of the downstream turbine. Based on approximated cross-stream velocity components of upstream wakes, the total turbine yaw angle γ is expressed by

$$\gamma = \gamma_{\text{turb}} + \gamma_{\text{eff}} \ , \tag{10}$$

where γ_{turb} is the rotor misalignment to the wind, and γ_{eff} is the effective yaw angle describing the effects of upstream generated vortices.

2.3 *Optimisation setup*

In the current work, static optimisation is performed on a 4×4 aligned farm layout with NREL-5MW turbines. The turbine spacing is set to 7 and 5 rotor diameters in the streamwise and cross-stream directions, respectively. For inflow conditions, an aligned flow is considered at 8m/s in 5% ambient turbulence intensity. Wind shear and veer are not included.

The optimisation goal is to select yaw misalignment set-points that maximise wind farm power production

$$\gamma_{\text{opt}} = \text{argmax}_{\gamma} \, G(\gamma) \ , \tag{11}$$

where $G(\gamma)$ is the wind farm power production normalised by farm power without yaw misalignment

$$G(\gamma) = P(\gamma)/P(0) \ , \tag{12}$$

and γ is the list of yaw angles for all turbines N in the wind farm

$$\gamma = [\gamma_1, \gamma_2, \dots, \gamma_N], \text{ with } -25^\circ \leq \gamma_i \leq 25^\circ \ . \tag{13}$$

Model/Algorithm	**Parameter**	**Parameter value**
Jensen	k	0.05
(Jimenez)	k_d	0.05
Multi-zone	k_e	0.05
(Jimenez)	$m_{e,q}$	[-0.5, 0.3, 1.0]
	$M_{u,q}$	[0.5, 1.0, 5.5]
	a_u	12.00
	b_u	1.30
	k_d	0.05
Gaussian - GCH	k_a	0.380
(Bastankhah)	k_b	0.004
	α	0.580
	β	0.077
	ϵ	0.2D
	ϕ	2.000
SLSQP	$ftol$	1e-16
	eps	0.01

Table 1: Parameters for wake and deflection models and SLSQP.

The optimisation algorithm used is the gradient-based Sequential Least SQuares Programming (SLSQP) method developed by Kraft (1988). SLSQP is the standard and recommended algorithm in the `FLORIS` framework. The parameters for SLSQP and wake and deflection models used in the presented work are shown in Table 1.

3 DISCUSSION OF RESULTS

In this section, results for the steady-state wake steering optimisation are presented. Figure 1 shows the model comparison for a 4×4 layout with an initial yaw angle for all turbines of 12°. Optimal yaw set-points for each turbine in the wind farm are shown in the left plot, while optimisation results in terms of the objective function are presented in the right plot.

Significant model discrepancies in wind farm power predictions for optimal set-points can be noticed. Given each wake model's computed optimal yaw angles, a maximum of 48% difference in power evaluations is observed. It is worth noting that, although Gaussian and GCH share the same self-similar Gaussian velocity distribution in their model formulations, the difference in optimal power prediction reaches 23% for the presented case.

As shown in the left plot of Figure 1, a change in the wake model can correspond to significantly different optimal yaw angle solutions for the same wind farm layout, atmospheric conditions, and initial yaw angles. These discrepancies in optimal decision variables between wake models can be attributed to the model formulations and the initialisation sensitivity of the gradient-based optimiser. The Jensen model nearly suggests no control action when compared to the aligned flow case, apart from a 2° optimal yaw angle for the second row of turbines. Due to the top-hat streamwise velocity distribution in the wake, the model is not capable of capturing wake steering power benefits until partial wake overlapping is reached with downstream turbines. This phenomenon is emphasised in the investigated case due to the turbine alignment in the wind farm layout. The Multi-zone model optimal solution is non-physical. By applying a yaw angle to the last row of turbines, no increase in wind farm power is expected. This phenomenon is attributed to the high sensitivity of the gradient-based optimiser to initialisation, as discussed later in this section. The Gaussian model suggests a 25° yaw angle, variable upper bound, for the first three rows in the farm layout, and no yaw actuation for the last row of turbines. Due to the ability to model secondary steering effects, the optimal set-points of the GCH model consist of a gradual decrease in the yaw angle per row, starting from 25° and ending at 0° for the last turbine row. As the effective yaw angle induced by the vortices generated by upstream turbines is captured, a lower rotor misalignment is required to achieve the same deflection in the wake.

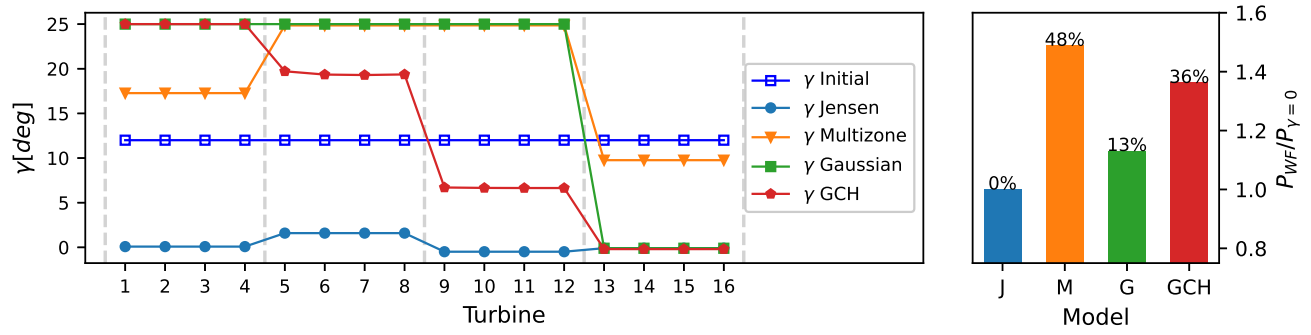

Figure 1: Model comparison for a 4×4 wind farm optimisation. Left plot: optimised set-points for each turbine, with 12° initial yaw angles. Dashed lines delimit wind farm rows. Right plot: Optimal normalised farm power value for each wake model. Turbine naming convention: turbine "1" at bottom-left, turbine "4" at top-left, turbine "13" at bottom-right, and turbine "16" at top-right.

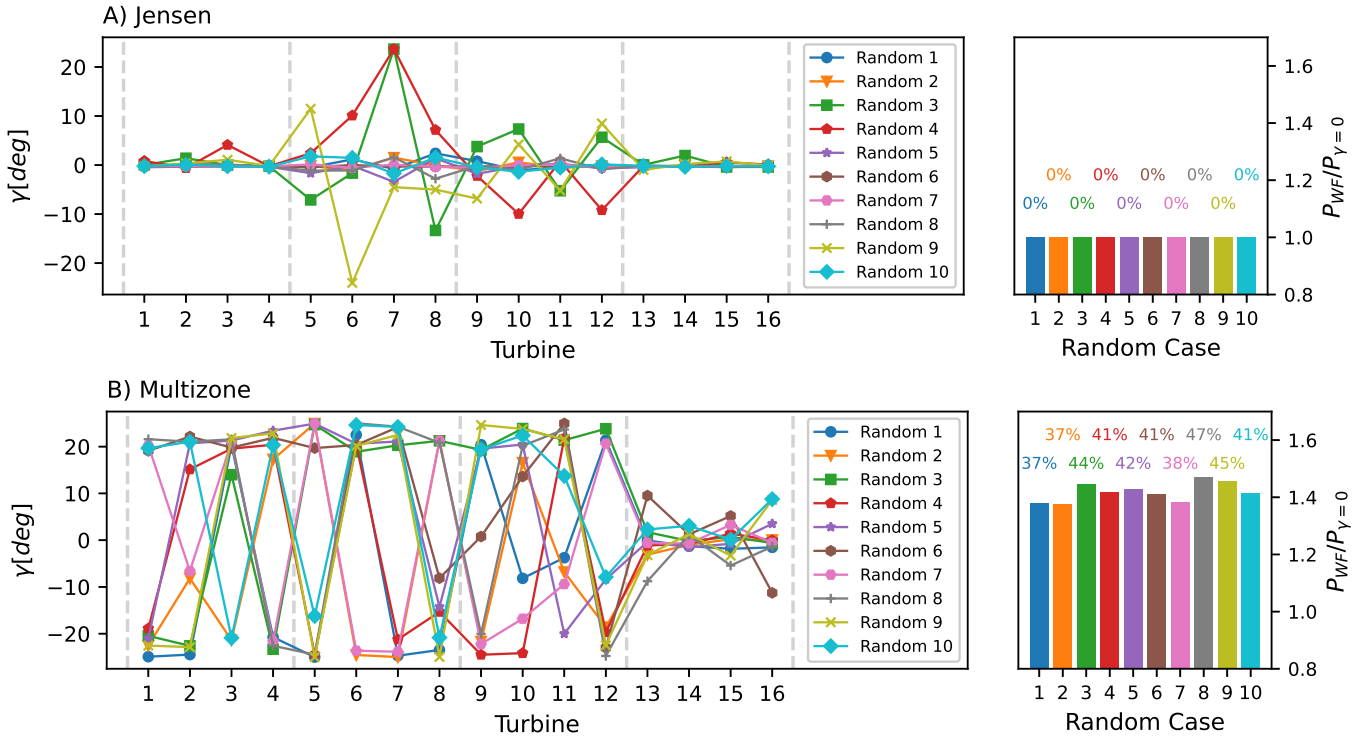

Figure 2: Initialisation sensitivity of a 4×4 wind farm optimisation for Jensen (**A**) and Multi-zone (**B**) models. Left plots: optimised set-points (yaw angles) for each turbine provided random sets "Random" of initial points. Dashed lines delimit wind farm rows. Right plots: Objective function (normalised farm power) optimised value for each random case of initial points. Turbine naming convention: turbine "1" at bottom-left, turbine "4" at top-left, turbine "13" at bottom-right, and turbine "16" at top-right.

The sensitivity of wake steering optimisation to initialisation when using a gradient-based optimiser is assessed for each wake model investigated. Ten random initial conditions are defined by randomly sampling ten independent sets of yaw angles from a uniform distribution on $[-25^{\circ}, +25^{\circ}]$. Random initialisation is representative of the unsteady and heterogeneous inflow conditions a wind farm might experience during operation. Figure 2 and Figure 3 show results for a 4×4 farm layout optimisation for Jensen and Multi-zone models, and Gaussian and GCH models, respectively. Left plots illustrate the resulting optimal yaw angles for each random initial condition, while right plots show the optimisation results in terms of the objective function.

A general sensitivity to initialisation when using a gradient-based optimisation algorithm can be observed. The presence of sub-optimal solutions can be clearly noticed, implying the presence of multiple local maxima in the wind farm power function. The Jensen model (Figure 2-A) shows some variations in the optimal solution depending on the initial yaw angles. The top-hat velocity distribution in the model formulation exhibits a sharp transition at the wake edges, leading to sudden variations in the power function. However, power variations in sub-optimal solutions are negligible due to the underprediction of streamwise velocity deficit in the investigated conditions. Additional results for a uniform inflow velocity of 4m/s show potential power losses due to sub-optimal solutions up to 14%.

The Multi-zone model (Figure 2-B) is highly sensitive to initialisation. Sub-optimal solutions lead to significant yaw-angle variations and up to 10% poten-

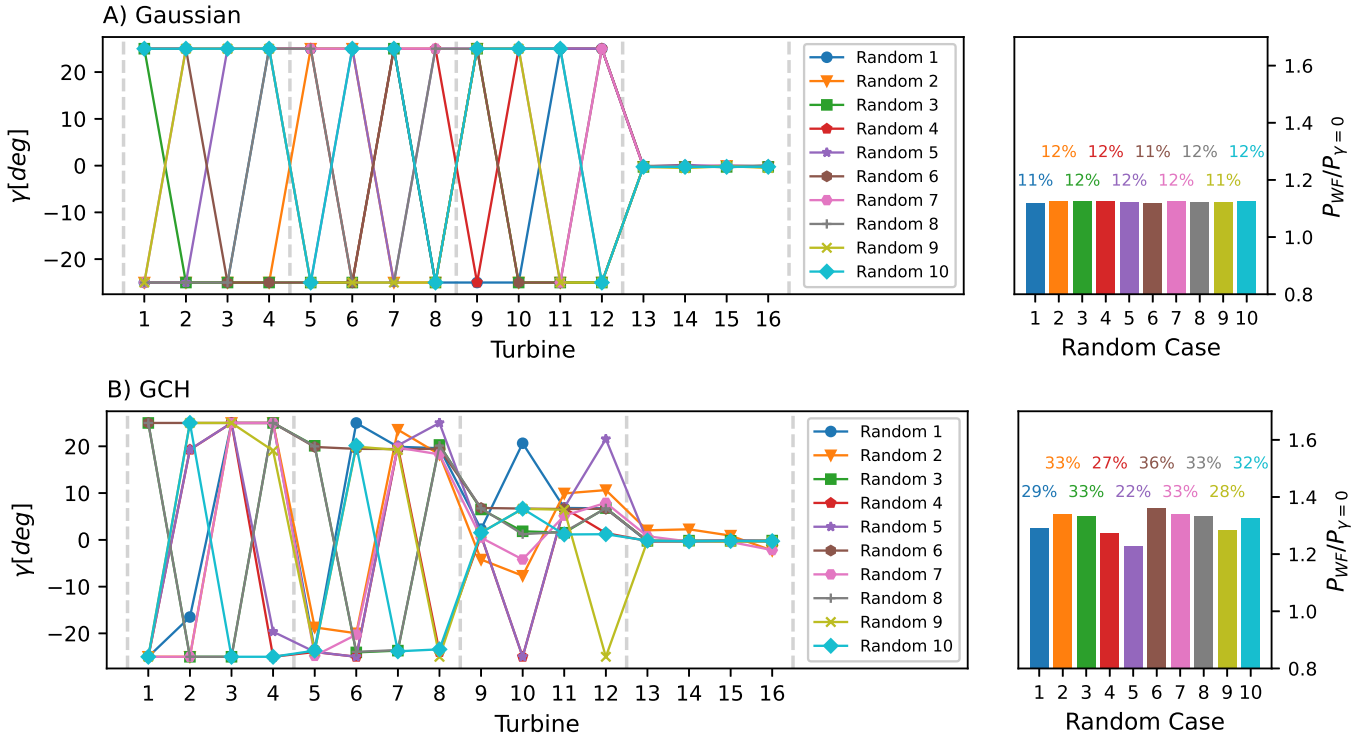

Figure 3: Initialisation sensitivity of a 4×4 wind farm optimisation for Gaussian (**A**) and GCH (**B**) models. Left plots: optimised set-points (yaw angles) for each turbine provided random sets "Random" of initial points. Dashed lines delimit wind farm rows. Right plots: Objective function (normalised farm power) optimised value for each random case of initial points. Turbine naming convention: turbine "1" at bottom-left, turbine "4" at top-left, turbine "13" at bottom-right, and turbine "16" at top-right.

tial power losses. The model formulation describes a top-hat velocity distribution for multiple zones within a turbine wake. The sharp interfaces between wake zones, as well as the surrounding flow, lead to a discontinuous, highly non-linear power function. The least sensitive model to initialisation is the Gaussian model (Figure 3-A), with potential power losses of 1% only. Sub-optimal solutions can be identified when upstream and downstream turbines alternate optimal yaw angles from positive to negative values and vice versa. Finally, (Figure 3-B) clearly shows the presence of multiple maxima in the GCH model power function. Although a smooth self-similar Gaussian distribution is applied to the streamwise velocity, as per the Gaussian wake model, the GCH power function exhibits multi-modality, leading to power variations in sub-optimal solutions up to 14% when using a gradient-based optimiser.

Overall, the Gaussian wake model can be identified as the least sensitive to initialisation. By considering the behaviour of the models in an optimisation prospective, hence not accounting for the accuracy of their physical modelling, Gaussian is the most suitable and reliable model for the investigated conditions, exhibiting the least overall variations in optimal yaw angles and resulting wind farm power improvements.

In the remainder of this section, a single specific case, "Test Case 1", is investigated in further depth. An additional random initialisation is generated by randomly sampling 16 yaw angles from a uniform distribution on $[-25°, +25°]$ and a static optimisation is

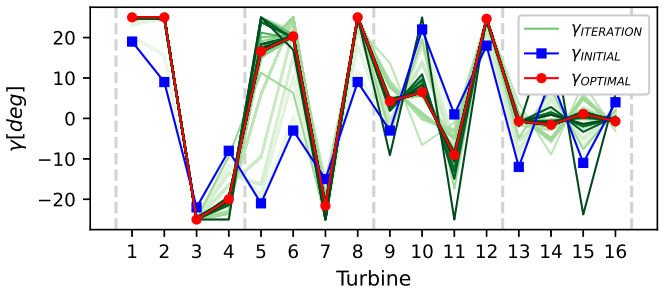

Figure 4: Optimised yaw angles (red) for each turbine provided a random set of initial points "Test Case 1" (blue). Optimiser farm evaluations are shown in green, with the lightest colour being the first iteration and the darkest one having reached convergence. Dashed lines delimit wind farm rows. Turbine naming convention: turbine "1" at bottom-left, turbine "4" at top-left, turbine "13" at bottom-right, and turbine "16" at top-right.

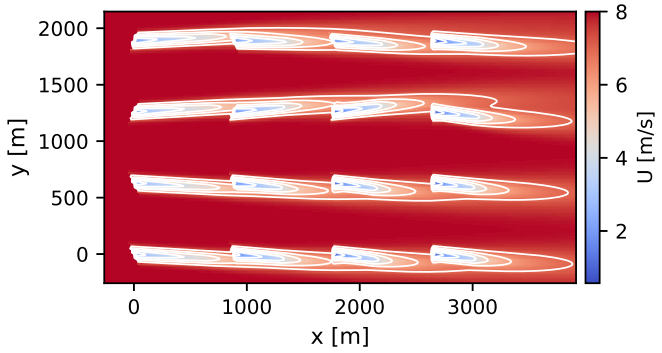

Figure 5: Streamwise velocity at hub height of the optimised layout for "Test Case 1". Turbine naming convention: turbine "1" at bottom-left, turbine "4" at top-left, turbine "13" at bottom-right, and turbine "16" at top-right.

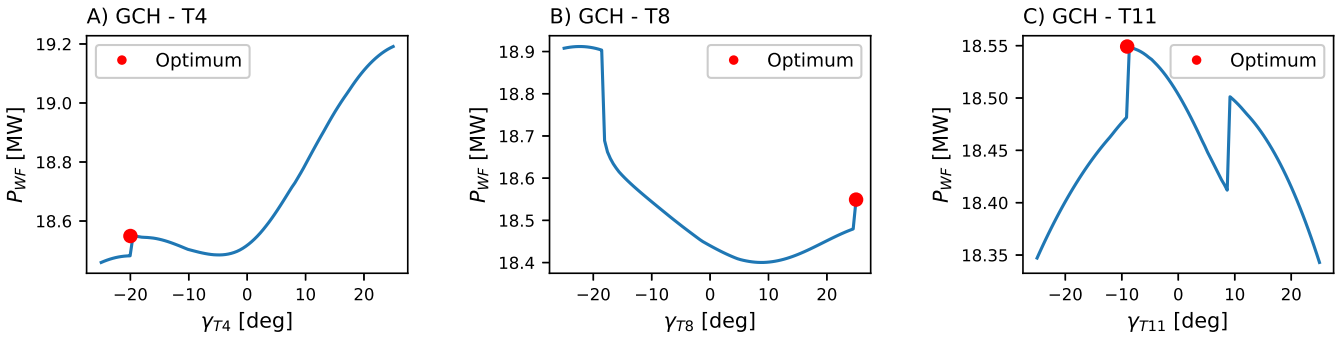

Figure 6: Wind farm power plots for (**A**) turbine 4 (T4), (**B**) turbine 8 (T8), and (**C**) turbine 11 (T11) yaw angles. Turbines are swept $\pm 25°$ with the optimised yaw angles as a starting point. SLSQP optimal solution is displayed in red. Turbine naming convention: turbine "1" at bottom-left, turbine "4" at top-left, turbine "13" at bottom-right, and turbine "16" at top-right.

conducted on a 4×4 farm layout using the GCH wake model. Initial and optimal yaw angles are shown in Figure 4, while the streamwise velocity at hub height of the optimised farm layout is illustrated in Figure 5.

As shown in Figure 5, the computed optimal set-points for the wind farm represent a sub-optimal solution. Given the inflow conditions and farm layout investigated, and the resulting optimal yaw angles, no significant aerodynamic interaction between farm columns of turbines is observed. By analysing the optimisation solution per column, the power extracted by the second, third and fourth columns of turbines is 1%, 3%, and 20% lower, respectively, than the first column.

Further analysis of the GCH farm power function is undertaken. The computed optimal turbine yaw settings are kept constant while the yaw angles for turbine 4 (last of the first row), 8 (last of the second row), and 11 (second-to-last of the third row) are varied from -25° to -25° (variable bounds) in steps of 0.1°. A comparison with the optimal set-points predicted by the SLSQP gradient-based optimisation is conducted. Results are illustrated in Figure 6.

Results clearly indicate the presence of local maxima as well as discontinuities in the power function for all turbines investigated. Discontinuities are attributed to the modelling of secondary steering effects within the GCH wake model formulation. As an upstream turbine's yaw angle is varied, the wake of a downstream turbine can experience a sudden change in deflection when overlapping with the influence zone of vortices generated upstream. While the SLSQP optimiser reached a global optimum solution for turbine 11, sub-optimal solutions are identified for turbines 4 and 8, questioning the suitability of employing a gradient-based optimiser in wake steering control.

4 CONCLUSIONS

This paper investigated the sensitivity of wake steering strategies to both the choice of analytical wake models and optimisation parameters. Static optimisation for power maximisation was conducted on a 4×4 wind farm layout using `FLORIS` framework, where different wake models were compared in terms of absolute power predictions and optimal decision variables. Results showed substantial discrepancies in absolute farm power predictions for optimal set-points, up to 48% for the investigated cases, and in optimal decision variables, with different or even opposite optimal yaw angle settings.

Initialisation sensitivity was assessed by performing optimisation with random sets of initial yaw angles. In the investigated conditions, solutions corresponding to local extrema led to potential power losses up to 14% compared to the global maximum for power production. Further analysis into the behaviour of the farm power function confirmed its multi-modal and discontinuous nature, suggesting that care must be taken when using gradient-based methods in wake steering optimisation.

Future work should broaden the range of wind farm conditions tested, including inflow variations in wind direction, wind speed, and turbulence intensity, as well as larger and more complex wind farm layouts. Furthermore, additional optimisation algorithms should be employed to assess further the sensitivity of wake steering strategies to optimiser choice.

REFERENCES

Abkar, M. & F. Porté-Agel (2015, March). Influence of atmospheric stability on wind-turbine wakes: A large-eddy simulation study. *Physics of Fluids 27*(3), 035104.

Archer, C. L., A. Vasel-Be-Hagh, C. Yan, S. Wu, Y. Pan, J. F. Brodie, & A. E. Maguire (2018, September). Review and evaluation of wake loss models for wind energy applications. *Applied Energy 226*, 1187–1207.

Barthelmie, R. J., K. Hansen, S. T. Frandsen, O. Rathmann, J. G. Schepers, W. Schlez, J. Phillips, K. Rados, A. Zervos, E. S. Politis, & P. K. Chaviaropoulos (2009, July). Modelling and measuring flow and wind turbine wakes in large wind farms offshore. *Wind Energy 12*(5), 431–444.

Barthelmie, R. J., S. C. Pryor, S. T. Frandsen, K. S. Hansen, J. G. Schepers, K. Rados, W. Schlez, A. Neubert, L. E. Jensen, & S. Neckelmann (2010, August). Quantifying the impact of wind turbine wakes on power output at offshore wind farms. *Journal of Atmospheric and Oceanic Technology 27*(8), 1302–1317.

Bastankhah, M. & F. Porté-Agel (2014, October). A new ana-

lytical model for wind-turbine wakes. *Renewable Energy 70*, 116–123.

Bastankhah, M. & F. Porté-Agel (2016, November). Experimental and theoretical study of wind turbine wakes in yawed conditions. *Journal of Fluid Mechanics 806*, 506–541.

Bastankhah, M., F. Porté-Agel, F. Port E-Agel, & . Affiliations (2019, March). Wind farm power optimization via yaw angle control: A wind tunnel study. *Journal of Renewable and Sustainable Energy 11*(2), 023301.

Bastankhah, M., C. R. Shapiro, S. Shamsoddin, D. F. Gayme, & C. Meneveau (2022, February). A vortex sheet based analytical model of the curled wake behind yawed wind turbines. *Journal of Fluid Mechanics 933*, 36.

Blondel, F. & M. Cathelain (2020, September). An alternative form of the super-Gaussian wind turbine wake model. *Wind Energy Science 5*(3), 1225–1236.

Campagnolo, F., V. Petrović, J. Schreiber, E. M. Nanos, A. Croce, & C. L. Bottasso (2016, September). wind tunnel testing of a closed-loop wake deflection controller for wind farm power maximization. *Journal of Physics: Conference Series 753*(3), 032006.

Dilip, D. & F. Porté-Agel (2017, May). Wind Turbine Wake Mitigation through Blade Pitch Offset. *Energies 2017, Vol. 10, Page 757 10*(6), 757.

Fleming, P., J. Annoni, M. Churchfield, L. A. Martinez-Tossas, K. Gruchalla, M. Lawson, & P. Moriarty (2018). A simulation study demonstrating the importance of large-scale trailing vortices in wake steering. *Wind Energ. Sci 3*, 243–255.

Fleming, P., J. Annoni, J. J. Shah, L. Wang, S. Ananthan, Z. Zhang, K. Hutchings, P. Wang, W. Chen, & L. Chen (2017). Field test of wake steering at an offshore wind farm. *Wind Energy Science 2*(1), 229–239.

Fleming, P., P. M. Gebraad, S. Lee, J. W. Van Wingerden, K. Johnson, M. Churchfield, J. Michalakes, P. Spalart, & P. Moriarty (2015, December). Simulation comparison of wake mitigation control strategies for a two-turbine case. *Wind Energy 18*(12), 2135–2143.

Frandsen, S., R. Barthelmie, S. Pryor, O. Rathmann, S. Larsen, J. Højstrup, & M. Thøgersen (2006). Analytical modelling of wind speed deficit in large offshore wind farms. *Wind Energy 9*, 39–53.

Gebraad, P. M., F. W. Teeuwisse, J. W. Van Wingerden, P. Fleming, S. D. Ruben, J. R. Marden, & L. Y. Pao (2014, June). A data-driven model for wind plant power optimization by yaw control. In *Proceedings of the American Control Conference*, pp. 3128–3134.

Gori, F., A. Wynn, & S. Laizet (2022). Sensitivity of Wind Farm Wake Steering Optimisation to Analytical Wake Models. *submitted to Wind Energy*.

Hegazy, A., F. Blondel, M. Cathelain, & S. Aubrun (2022, January). LiDAR and SCADA data processing for interacting wind turbine wakes with comparison to analytical wake models. *Renewable Energy 181*, 457–471.

Houck, D. R. (2021). Review of wake management techniques for wind turbines. *Wind Energy 25*(2), 195–220.

Howland, M. F., S. K. Lele, & J. O. Dabiri (2019). Wind farm power optimization through wake steering. *Proceedings of the National Academy of Sciences of the United States of America 116*(29), 14495–14500.

Jensen, N. (1983). A note on wind generator interaction. Technical Report RISO-M-2411, Risoe National Laboratory, Roskilde (Denmark).

Jiménez, Á., A. Crespo, & E. Migoya (2009, December). Application of a LES technique to characterize the wake deflection of a wind turbine in yaw. *Wind Energy 13*(6), 559–572.

Katic, I., J. Højstrup, & N. Jensen (1987). A Simple Model for Cluster Efficiency. *EWEC'86. Proceedings 1*, 407–410.

Kheirabadi, A. C. & R. Nagamune (2019, September). A quantitative review of wind farm control with the objective of wind farm power maximization. *Journal of Wind Engineering and Industrial Aerodynamics 192*, 45–73.

King, J., P. Fleming, R. N. King, L. A. Martínez-Tossas, C. Bay, R. Mudafort, & E. Simley (2021). Control-oriented model for secondary effects of wake steering. *Wind Energy Science 6*(3), 701–714.

Kraft, D. (1988). *A software package for sequential quadratic programming* (28 ed.), Volume 88 of *Deutsche Forschungs- und Versuchsanstalt für Luft- und Raumfahrt Köln: Forschungsbericht*. Wiss. Berichtswesen d. DFVLR.

Niayifar, A. & F. Porté-Agel (2016, September). Analytical Modeling of Wind Farms: A New Approach for Power Prediction. *Energies 9*(9), 741.

Nilsson, K., S. Ivanell, K. S. Hansen, R. Mikkelsen, J. N. Sørensen, S. Breton, & D. Henningson (2015, March). Large-eddy simulations of the Lillgrund wind farm. *Wind Energy 18*(3), 449–467.

Nygaard, N. G. (2014). Wakes in very large wind farms and the effect of neighbouring wind farms. *Journal of Physics: Conference Series 524*(1), 0–10.

Qian, G. & T. Ishihara (2018, March). A New Analytical Wake Model for Yawed Wind Turbines. *Energies 11*(3), 665.

Schreiber, J., A. Balbaa, & C. L. Bottasso (2020, February). Brief communication: A double-Gaussian wake model. *Wind Energy Science 5*(1), 237–244.

Shapiro, C. R., D. F. Gayme, & C. Meneveau (2018, April). Modelling yawed wind turbine wakes: A lifting line approach. *Journal of Fluid Mechanics 841*, R11–R112.

Shapiro, C. R., D. F. Gayme, & C. Meneveau (2020). Generation and decay of counter-rotating vortices downstream of yawed wind turbines in the atmospheric boundary layer. *Journal of Fluid Mechanics 903*, 2.

Stieren, A. & R. Stevens (2021, June). Evaluating wind farm wakes in large eddy simulations and engineering models. *Journal of Physics: Conference Series 1934*(1), 11.

Yang, P. & H. Najafi (2021). The Effect of Using Different Wake Models on Wind Farm Layout Optimization: A Comparative Study. *Journal of Energy Resources Technology 144*(7), 9.

Zong, H. & F. Porté-Agel (2020). A momentum-conserving wake superposition method for wind farm power prediction. *Journal of Fluid Mechanics 889*, 15.